

---

# COMPOUNDE: KNOWLEDGE GRAPH EMBEDDING WITH TRANSLATION, ROTATION AND SCALING COMPOUND OPERATIONS

---

**Xiou Ge**

University of Southern California  
Los Angeles, USA  
xiouge@usc.edu

**Yun-Cheng Wang**

University of Southern California  
Los Angeles, USA  
yunchenw@usc.edu

**Bin Wang**

National University of Singapore  
Singapore  
bwang28c@gmail.com

**C.-C. Jay Kuo**

University of Southern California  
Los Angeles, USA  
cckuo@sipi.usc.edu

## ABSTRACT

Translation, rotation, and scaling are three commonly used geometric manipulation operations in image processing. Besides, some of them are successfully used in developing effective knowledge graph embedding (KGE) models such as TransE and RotatE. Inspired by the synergy, we propose a new KGE model by leveraging all three operations in this work. Since translation, rotation, and scaling operations are cascaded to form a compound one, the new model is named CompoundE. By casting CompoundE in the framework of group theory, we show that quite a few scoring-function-based KGE models are special cases of CompoundE. CompoundE extends the simple distance-based relation to relation-dependent compound operations on head and/or tail entities. To demonstrate the effectiveness of CompoundE, we conduct experiments on three popular KG completion datasets. Experimental results show that CompoundE consistently achieves the state-of-the-art performance.

**Keywords** Knowledge graph embedding · Compounding Operations

## 1 Introduction

Knowledge graphs (KGs) such as DBpedia [1], YAGO [2], NELL [3], Wikidata [4], Freebase [5], and ConceptNet [6] have been created and made available to the public to facilitate research on KG modeling and applications. KG representation learning, also known as knowledge graph embedding (KGE), has been intensively studied in recent years. Yet, it remains to be one of the most fundamental problems in Artificial Intelligence (AI) and Data Engineering research. KGE is critical to many downstream applications such as multihop reasoning [7, 8], KG alignment [9, 10], entity classification [11], etc.

Triples, denoted by  $(h, r, t)$ , are basic elements of a KG, where  $h$  and  $t$  are head and tail entities while  $r$  is the relation connecting them. For instance, the fact “Los Angeles is located in the USA” can be encoded as a triple (Los Angeles, **isLocatedIn**, USA). The link prediction (or KG completion) task is often used to evaluate the effectiveness of KGE models. That is, the task is to predict  $t$  with given  $h$  and  $r$ , or to predict  $h$  with given  $r$  and  $t$ . KGE models are evaluated based on how well the prediction matches the ground truth.

There are several challenges in the design of good KGE models. First, real-world KGs often contain a large number of entities. It is impractical to have high-dimensional embeddings due to device memory constraints. Yet, the performance of KGE models may deteriorate significantly in low-dimensional settings. How to design a KGE model that is effective in low-dimensional settings is not trivial. Second, complex relation types (e.g., hierarchical relations, surjective relations, antisymmetric relations, etc.) remain difficult to model. The link prediction performance for 1-N, N-1, and N-N

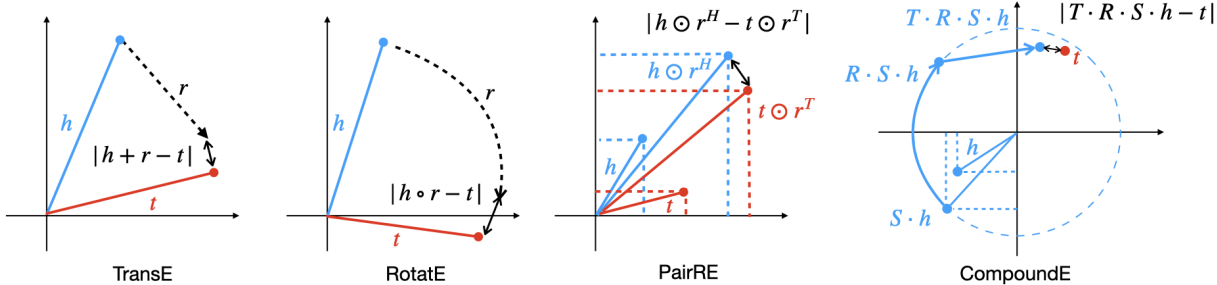


Figure 1: An illustration of previous distance-based KGE models and CompoundE.

relations is challenging for many existing KGE models. The relation “isLocatedIn” is an example of a N-1 relation. Since there are many cities other than “Los Angeles” also located in the USA, it is not easy to encode these relations effectively. Third, each of extant KGE models has its own strengths and weaknesses. It is desired yet unclear how to design a KGE model that leverages strengths of some models and complements weaknesses of others.

Geometric manipulation operations such as translation and rotation have been used to build effective knowledge graph embedding (KGE) models (e.g., TransE, RotatE). Inspired by their success, we look for generalized geometric manipulations in image processing [12]. To this end, translation, rotation, and scaling are three common geometric manipulation operations. Furthermore, they can be cascaded to yield a generic compound operation that finds numerous applications. Examples include image warping [13], image morphing [14], and robot motion planning [15]. Motivated by the synergy, we propose a new KGE model to address the above-mentioned challenges. Since translation, rotation, and scaling operations are cascaded to form a compound operation, the proposed KGE model is named CompoundE. Compound operations inherit many desirable properties from the affine group, allowing CompoundE to model complex relations in different KGs. Moreover, since geometric transformations can be composed in any order, CompoundE has a large number of design variations to choose from. One can select the optimal CompoundE variant that best suits the characteristics of an individual dataset.

There are four main contributions of this work. They are summarized below.

- We present a novel KG embedding model called CompoundE, which combines three fundamental operations in the affine group and offers a wide range of designs.
- It is proved mathematically that CompoundE can handle complex relation types in KG thanks to unique properties of the affine group.
- We conduct extensive experiments on three popular KG completion datasets; namely FB15k-237, WN18RR, and ogbl-wikikg2. Experimental results show that CompoundE achieves state-of-the-art performance.
- Against large-scale datasets containing millions of entities under the memory constraint, CompoundE outperforms other benchmarking methods by a big margin with fewer parameters.

The rest of this paper is organized as follows. Recent KGE models for both distance-based and semantic matching-based categories are first reviewed in Section 2. Then, we present CompoundE, show its relationship with previous KG embedding models, and explain the reason why it can model complex relations well in Section 3. Versatile transformations introduced by CompoundE lead to better performance. To demonstrate its effectiveness, we conduct extensive experiments on the link prediction task in Section 4. Finally, concluding remarks are given and possible extensions are suggested in Section 5.

## 2 Related Work

### 2.1 Distance-based Models

The distance-based strategy offers a popular methodology in developing KGE models. The main idea is to model a relation as a transformation that places head entity vectors in the proximity of their corresponding tail entity vectors, and vice versa. For a given triple,  $(h, r, t)$ , the goal is to minimize the distance between  $h$  and  $t$  vectors after the transformation introduced by  $r$ . TransE [16] is one of the earlier KGE models that interpret relations between entities as translation operations in the vector space. Drawbacks of TransE include inability to model one-to-many, many-to-one, many-to-many, and symmetric relations. RotatE [17] models entities in the complex vector space and

interprets a relation as a rotation instead of a translation. The self-adversarial negative sampling contributes to RotatE’s performance improvement as compared to its predecessors. Instead of rotating heads to match tails, PairRE [18] performs transformations on both heads and tails. Specifically, head and tail entities had a Hadamard product with their respective weight vectors  $r^H$  and  $r^T$ . This elementwise multiplication is nothing but the scaling operation. LinearRE [19] offers a similar model but adds a translation component between the scaled head and tail entities. TorusE [20] projects embedding in an  $n$ -dimensional torus space and optimizes the generalized translation-based embedding. MuRP [21] and ROTH [22] leverage the power of hyperbolic geometry to better model the hierarchical structure in KGs.

## 2.2 Semantic-Matching-based Models

Another related idea of developing KGE models is to measure the semantic matching score. RESCAL [23] adopts a bilinear scoring function as the objective in solving a three-way rank- $r$  matrix factorization problem. DistMult [24] also uses a bilinear scoring function but enforces the relation embedding matrix to be diagonal. ANALOGY [25] demands the relation embedding matrix to be orthonormal and commutative by imposing regularization constraints. ComplEx [26] extends the bilinear product score to the complex vector space so as to model antisymmetric relations more effectively. Simple [27] and TuckER [28] further model 3D tensor factorization with Canonical Polyadic decomposition and Tucker decomposition, respectively. QuatE [29] and DualE [30] extends from the complex representation to the hypercomplex representation with 4 degrees of freedom to gain more expressive rotational capability.

## 2.3 Classifier-based Models

Another popular approach to build KGE models is based on the classification framework. For example, a Multilayer Perceptron (MLP) [31] is used to measure the likelihood of unseen triples for link prediction. NTN [32] adopts a bilinear tensor neural layer to model interactions between entities and relations of triples. ConvE [33] reshapes and stacks the head entity and the relation vector to form a 2D shape data, applies Convolutional Neural Networks (CNNs) to extract features, and uses extracted features to interact with tail embedding. R-GCN [34] applies a Graph Convolutional Network (GCN) and considers the neighborhood of each entity equally. CompGCN [35] performs a composition operation over each edge in the neighborhood of a central node. The composed embeddings are then convolved with specific filters representing the original and the inverse relations, respectively. M-DCN [36] adopts a multi-scale dynamic convolutional network to model complex relations such as 1-N, N-1, and N-N relations. All the above mentioned examples are based on neural networks. Yet, there is a non-neural-network classification method, called KGBoost [37], developed recently. KGBoost proposes a novel negative sampling method and uses the XGBoost classifier for link prediction.

## 2.4 Entity-Transformation-based Models

Another line of work attempts to improve baseline models such as TransE by adding a relation-specific transformation. TransH [38] enables the relation-specific entity representation by projecting each entity to a relation-specific hyperplane. TransR [39] models relations and entities in two different spaces. TransD [40] comes up with dynamic mapping matrices using relation and entity projection vectors. TransSparse [41] enforces the relation projection matrix to be sparse. SFBR [42] introduces a semantic filter that includes a scaling and shift component. ReflectE [43] models a relation as the Householder reflection.

# 3 Method

Translation, rotation, and scaling transformations appear frequently in engineering applications. In image processing, a cascade of translation, rotation, and scaling operations offers a set of image manipulation techniques. Such compound operations can be used to develop a new KGE model called CompoundE. We define CompoundE in Section 3.1, explain that it belongs to the affine group in Section 3.2, and show that it is a generalized form of TransE, RotatE, PairRE, and a few other distance-based embedding models in Section 3.3. Furthermore, we discuss the properties of CompoundE in Section 3.4.

## 3.1 Definition of CompoundE

Three forms of CompoundE scoring function can be written as

- CompoundE-Head

$$f_r(h, t) = \|\mathbf{T}_r \cdot \mathbf{R}_r \cdot \mathbf{S}_r \cdot \mathbf{h} - \mathbf{t}\|, \quad (1)$$

- CompoundE-Tail

$$f_r(h, t) = \|\mathbf{h} - \hat{\mathbf{T}}_r \cdot \hat{\mathbf{R}}_r \cdot \hat{\mathbf{S}}_r \cdot \mathbf{t}\|, \quad (2)$$

- CompoundE-Full

$$f_r(h, t) = \|\mathbf{T}_r \cdot \mathbf{R}_r \cdot \mathbf{S}_r \cdot \mathbf{h} - \hat{\mathbf{T}}_r \cdot \hat{\mathbf{R}}_r \cdot \hat{\mathbf{S}}_r \cdot \mathbf{t}\|, \quad (3)$$

where  $\mathbf{h}$ ,  $\mathbf{t}$  denote head and tail entity embeddings,  $\mathbf{T}_r$ ,  $\mathbf{R}_r$ ,  $\mathbf{S}_r$  denote the translation, rotation, and scaling operations for the head entity embedding, and  $\hat{\mathbf{T}}_r$ ,  $\hat{\mathbf{R}}_r$ ,  $\hat{\mathbf{S}}_r$  denote the counterparts for the tail entity embedding, respectively. These constituent operators are relation-specific. To generalize, any order or subset of translation, rotation, and scaling component can be a valid instance of CompoundE. Since matrix multiplications are non-commutative, different orders of cascading the constituent operators result in distinct CompoundE operators. We illustrate different ways of cascading geometric transformations to compose distinct CompoundE operators in Fig. 6 of the appendix.

We follow RotatE’s negative sampling loss and the self-adversarial training strategy. The loss function of CompoundE can be written as

$$L_{\text{KGE}} = -\log \sigma(\zeta_1 - f_r(h, t)) - \sum_{i=1}^n p(h'_i, r, t'_i) \log \sigma(f_r(h'_i, t'_i) - \zeta_1), \quad (4)$$

where  $\sigma$  is the sigmoid function,  $\zeta_1$  is a fixed margin hyperparameter,  $(h'_i, r, t'_i)$  is the  $i$ th negative triple, and  $p(h'_i, r, t'_i)$  is the probability of drawing negative triple  $(h'_i, r, t'_i)$ . Given a positive triple,  $(h_i, r, t_i)$ , the negative sampling distribution is

$$p(h'_j, r, t'_j | \{(h_i, r, t_i)\}) = \frac{\exp \alpha_1 f_r(h'_j, t'_j)}{\sum_i \exp \alpha_1 f_r(h'_i, t'_i)}, \quad (5)$$

where  $\alpha_1$  is the temperature of sampling.

### 3.2 CompoundE As An Affine Group

Most analysis in previous work [44] was restricted to the Special Euclidean Group  $\mathbf{SE}(n)$ . Yet, we will show that CompoundE is not a special Euclidean group but an affine group. To proceed, we need to introduce the lie group and three special groups formally below.

**Definition 3.1.** *A Lie group is a continuous group that is also a differentiable manifold.*

Several Lie group examples are given below.

- The real vector space,  $\mathbb{R}^n$ , with the canonical addition as the group operation.
- The real vector space excluding zero,  $(\mathbb{R} \setminus \{0\})$ , with the element-wise multiplication as the group operation.
- The general linear group,  $GL_n(\mathbb{R})$ , with the the canonical matrix multiplication as the group operation.

Furthermore, the following three special groups are commonly used.

**Definition 3.2.** *The special orthogonal group is defined as*

$$\mathbf{SO}(n) = \left\{ \mathbf{A} \in \mathbf{GL}_n(\mathbb{R}) \mid \mathbf{A}^T \mathbf{A} = \mathbf{I} \wedge \det \mathbf{A} = 1 \right\}. \quad (6)$$

**Definition 3.3.** *The special Euclidean group is defined as*

$$\mathbf{SE}(n) = \left\{ \mathbf{A} \mid \mathbf{A} = \begin{bmatrix} \mathbf{R} & \mathbf{v} \\ \mathbf{0} & 1 \end{bmatrix}, \mathbf{R} \in \mathbf{SO}(n), \mathbf{v} \in \mathbb{R}^n \right\}. \quad (7)$$

**Definition 3.4.** *The affine group is defined as*

$$\mathbf{Aff}(n) = \left\{ \mathbf{M} \mid \mathbf{M} = \begin{bmatrix} \mathbf{A} & \mathbf{v} \\ \mathbf{0} & 1 \end{bmatrix}, \mathbf{A} \in \mathbf{GL}_n(\mathbb{R}), \mathbf{v} \in \mathbb{R}^n \right\}. \quad (8)$$

By comparing Eqs. (7) and (8), we see that  $\mathbf{SE}(n)$  is a subset of  $\mathbf{Aff}(n)$ .

Without loss of generality, consider  $n = 2$ . If  $\mathbf{M} \in \mathbf{Aff}(2)$ , we have

$$\mathbf{M} = \begin{bmatrix} \mathbf{A} & \mathbf{v} \\ \mathbf{0} & 1 \end{bmatrix}, \mathbf{A} \in \mathbb{R}^{2 \times 2}, \mathbf{v} \in \mathbb{R}^2. \quad (9)$$

The 2D translational matrix can be written as

$$\mathbf{T} = \begin{bmatrix} 1 & 0 & v_x \\ 0 & 1 & v_y \\ 0 & 0 & 1 \end{bmatrix}, \quad (10)$$

while the 2D rotational matrix can be expressed as

$$\mathbf{R} = \begin{bmatrix} \cos(\theta) & -\sin(\theta) & 0 \\ \sin(\theta) & \cos(\theta) & 0 \\ 0 & 0 & 1 \end{bmatrix}. \quad (11)$$

It is easy to verify that they are both special Euclidean groups (i.e.  $\mathbf{T} \in \mathbf{SE}(2)$  and  $\mathbf{R} \in \mathbf{SE}(2)$ ). On the other hand, the 2D scaling matrix is in form of

$$\mathbf{S} = \begin{bmatrix} s_x & 0 & 0 \\ 0 & s_y & 0 \\ 0 & 0 & 1 \end{bmatrix}. \quad (12)$$

It is not a special Euclidean group but an affine group of  $n = 2$  (i.e.,  $\mathbf{S} \in \mathbf{Aff}(2)$ ).

Compounding translation and rotation operations, we can get a transformation in the special Euclidean group,

$$\begin{aligned} \mathbf{T} \cdot \mathbf{R} &= \begin{bmatrix} 1 & 0 & v_x \\ 0 & 1 & v_y \\ 0 & 0 & 1 \end{bmatrix} \begin{bmatrix} \cos(\theta) & -\sin(\theta) & 0 \\ \sin(\theta) & \cos(\theta) & 0 \\ 0 & 0 & 1 \end{bmatrix} \\ &= \begin{bmatrix} \cos(\theta) & -\sin(\theta) & v_x \\ \sin(\theta) & \cos(\theta) & v_y \\ 0 & 0 & 1 \end{bmatrix} \in \mathbf{SE}(2). \end{aligned} \quad (13)$$

Yet, if we add the scaling operation, the compound will belong to the Affine group. One of such compound operator can be written as

$$\begin{aligned} \mathbf{T} \cdot \mathbf{R} \cdot \mathbf{S} &= \begin{bmatrix} 1 & 0 & t_x \\ 0 & 1 & t_y \\ 0 & 0 & 1 \end{bmatrix} \begin{bmatrix} \cos(\theta) & -\sin(\theta) & 0 \\ \sin(\theta) & \cos(\theta) & 0 \\ 0 & 0 & 1 \end{bmatrix} \begin{bmatrix} s_x & 0 & 0 \\ 0 & s_y & 0 \\ 0 & 0 & 1 \end{bmatrix} \\ &= \begin{bmatrix} s_x \cos(\theta) & -s_y \sin(\theta) & v_x \\ s_x \sin(\theta) & s_y \cos(\theta) & v_y \\ 0 & 0 & 1 \end{bmatrix} \in \mathbf{Aff}(2). \end{aligned} \quad (14)$$

When  $s_x \neq 0$  and  $s_y \neq 0$ , the compound operator is invertible. It can be written in form of

$$\mathbf{M}^{-1} = \begin{bmatrix} \mathbf{A}^{-1} & -\mathbf{A}^{-1}\mathbf{v} \\ \mathbf{0} & 1 \end{bmatrix}. \quad (15)$$

### 3.3 Relation with Other Distance-based KGE Models

CompoundE is actually a general form of quite a few distance-based KGE models. That is, we can derive their scoring functions from that of CompoundE by setting translation, scaling, and rotation operations to certain forms. Four examples are given below.

**Derivation of TransE.** We begin with CompoundE-Head and set its rotation component to identity matrix  $\mathbf{I}$  and scaling parameters to  $\mathbf{1}$ . Then, we get the scoring function of TransE as

$$f_r(h, t) = \|\mathbf{T}_r \cdot \mathbf{I} \cdot \text{diag}(\mathbf{1}) \cdot \mathbf{h} - \mathbf{t}\| = \|\mathbf{h} + \mathbf{r} - \mathbf{t}\|. \quad (16)$$

**Derivation of RotatE.** We can derive the scoring function of RotatE from CompoundE-Head by setting the translation component to  $\mathbf{I}$  (translation vector  $\mathbf{t} = \mathbf{0}$ ) and scaling component to  $\mathbf{1}$ .

$$f_r(h, t) = \|\mathbf{I} \cdot \mathbf{R}_r \cdot \text{diag}(\mathbf{1}) \cdot \mathbf{h} - \mathbf{t}\| = \|\mathbf{h} \circ \mathbf{r} - \mathbf{t}\|. \quad (17)$$

**Derivation of PairRE.** CompoundE-Full can be reduced to PairRE by setting both translation and rotation component to  $\mathbf{I}$ , for both head and tail transformation.

$$f_r(h, t) = \|\mathbf{I} \cdot \mathbf{I} \cdot \mathbf{S}_r \cdot \mathbf{h} - \mathbf{I} \cdot \mathbf{I} \cdot \hat{\mathbf{S}}_r \cdot \mathbf{t}\| = \|\mathbf{h} \odot \mathbf{r}^{\mathbf{H}} - \mathbf{t} \odot \mathbf{r}^{\mathbf{T}}\|. \quad (18)$$

**Derivation of LinearRE.** We can add back the translation component for the head transformation:

$$f_r(h, t) = \|\mathbf{T}_r \cdot \mathbf{I} \cdot \mathbf{S}_r \cdot \mathbf{h} - \mathbf{I} \cdot \mathbf{I} \cdot \hat{\mathbf{S}}_r \cdot \mathbf{t}\| = \|\mathbf{h} \odot \mathbf{r}^{\mathbf{H}} + \mathbf{r} - \mathbf{t} \odot \mathbf{r}^{\mathbf{T}}\|. \quad (19)$$

### 3.4 Properties of CompoundE

CompoundE has a richer set of operations and, therefore, it is more powerful than previous KGE models in modeling complex relations such as 1-to-N, N-to-1, and N-to-N relations in KG datasets. Modeling these relations are important since more than 98% of triples in FB15k-237 and WN18RR datasets involves complex relations. The importance of complex relations modeling is illustrated by two examples below. First, there is a need to distinguish different outcomes of relation compositions when modeling non-commutative relations. That is  $r_1 \cdot r_2 \rightarrow r_3$  while  $r_2 \cdot r_1 \rightarrow r_4$ . For instance,  $r_1, r_2, r_3$  and  $r_4$  denote **isFatherOf**, **isMotherOf**, **isGrandfatherOf** and **isGrandmotherOf**, respectively. TransE and RotatE cannot make such distinction since they are based on commutative relation embeddings. Second, to capture the hierarchical structure of relations, it is essential to build a good model for sub-relations. For example,  $r_1$  and  $r_2$  denote **isCapitalCityOf** and **cityLocatedInCountry**, respectively. Logically, **isCapitalCityOf** is a sub-relation of **cityLocatedInCountry** because if  $(h, r_1, t)$  is true, then  $(h, r_2, t)$  must be true. We will prove that CompoundE is capable of modeling symmetric/antisymmetric, inversion, transitive, commutative/non-commutative, and sub-relations in Section 6.3 of the appendix.

Table 1: Filtered ranking of link prediction on ogbl-wikikg2.

Datasets	ogbl-wikikg2		
	Dim	Valid MRR	Test MRR
AutoSF+NodePiece	-	0.5806	0.5703
ComplEx-RP	50	<u>0.6561</u>	<u>0.6392</u>
TransE	500	0.4272	0.4256
DistMult	500	0.3506	0.3729
ComplEx	250	0.3759	0.4027
RotatE	250	0.4353	0.4353
PairRE	200	0.5423	0.5208
TripleRE	200	0.6045	0.5794
CompoundE	100	<b>0.6704</b>	<b>0.6515</b>

Table 2: Filtered ranking of link prediction for FB15k-237 and WN18RR.

Datasets	FB15K-237				WN18RR			
	MRR	Hit@1	Hit@3	Hit@10	MRR	Hit@1	Hit@3	Hit@10
TransE [16]	0.294	-	-	0.465	0.226	-	-	0.501
DistMult [24]	0.241	0.155	0.263	0.419	0.430	0.390	0.440	0.490
ComplEx [26]	0.247	0.158	0.275	0.428	0.440	0.410	0.460	0.510
RotatE [17]	0.338	0.241	0.375	0.533	0.476	0.428	0.492	0.571
TorusE [45]	0.316	0.217	0.335	0.484	0.453	0.422	0.464	0.512
Tucker [28]	0.358	0.266	0.394	0.544	0.470	0.443	0.482	0.526
AutoSF [46]	0.360	0.267	-	<u>0.552</u>	0.490	0.451	-	0.567
RotatE3D [47]	0.347	0.250	0.385	0.543	0.489	0.442	<u>0.505</u>	<b>0.579</b>
MQuadE [48]	0.356	0.260	0.392	0.549	-	-	-	-
PairRE [18]	0.351	0.256	0.387	0.544	-	-	-	-
M-DCN [36]	0.345	0.255	0.380	0.528	0.475	0.440	0.485	0.540
GIE [44]	<u>0.362</u>	<u>0.271</u>	<u>0.401</u>	<u>0.552</u>	<u>0.491</u>	<b>0.452</b>	<u>0.505</u>	0.575
ReflectE [43]	0.358	0.263	0.396	0.546	0.488	0.450	0.501	0.559
CompoundE	<b>0.367</b>	<b>0.275</b>	<b>0.402</b>	<b>0.555</b>	<b>0.493</b>	<u>0.451</u>	<b>0.507</b>	<u>0.578</u>

## 4 Experiments

**Datasets.** We conduct experiments on three widely used benchmarking datasets: ogbl-wikikg2, FB15k-237, and WN18RR. ogbl-wikikg2 is a challenging Open Graph Benchmark dataset [49] extracted from the Wikidata [4] KG. Its challenge is to design embedding models that can scale to large KGs. FB15k-237 and WN18RR are extracted from the Freebase [5] and the WordNet [50], respectively. Inverse relations are removed from both to avoid the data

leakage problem. Their main challenge lies in modeling symmetry/antisymmetry and composition relation patterns. The detailed statistics of the three datasets are shown in Table 5 of the appendix.

**Evaluation Protocol.** To evaluate the link prediction performance of CompoundE, we compute the rank of the ground truth entity in the list of top candidates. Since embedding models tend to rank entities observed in the training set higher, we compute the filtered rank to prioritize candidates that would result in unseen triples. We follow the convention and adopt the Mean Reciprocal Rank (MRR) and Hits@ $k$  metrics to compare the quality of different KGE models. Higher MRR and H@ $k$  values indicate better model performance.

**Performance Benchmarking.** Tables 1 and 2 show the best performance of CompoundE and other benchmarking models for ogbl-wikikg2 and FB15k-237/WN18RR datasets, respectively. The best results are shown in bold fonts. CompoundE consistently outperforms all benchmarking models across all three datasets. As shown in Table 1, the results of CompoundE are much better than previous KGE models while the embedding dimension and the model parameter numbers are significantly lower for the ogbl-wikikg2 dataset. This implies lower computation and memory costs of CompoundE. We see from Table 2 that CompoundE has achieved significant improvement over distance-based KGE models using a single operation, either translation (TransE), rotation (RotatE), or scaling (PairRE). This confirms that cascading geometric transformations is an effective strategy for designing KG embeddings.

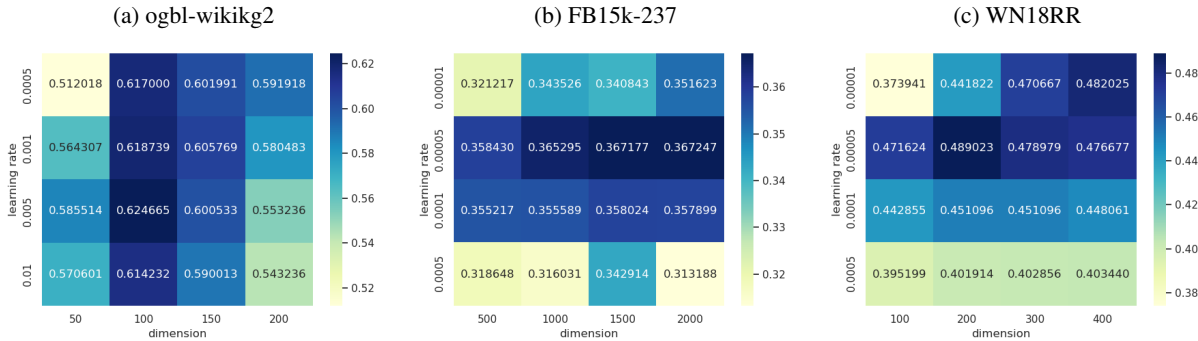


Figure 2: Heatmap of test MRR scores obtained from learning rate and dimension grid search.

**Hyperparameter Tuning.** We conduct two sets of controlled experiments to find the best model configurations for FB15k-237, WN18RR, and ogbl-wikikg2 datasets. For the first set, we evaluate the effect of different combinations of learning rates and embedding dimensions while keeping the batch size, the negative sample size, and other parameters constant. For the second set, we evaluate the effect of different combinations of the training batch size and the negative sample size, while keeping the learning rate, the embedding dimension, and other parameters constant. Figs. 2 (a)-(c) show MRR scores of CompoundE under different learning rates and embedding dimension settings, for ogbl-wikikg2, FB15k-237, and WN18RR, respectively. We see that CompoundE does not require a higher embedding dimension to achieve the optimal performance, indicating that its model size can be small. This is attractive for training and inference on mobile/edge devices with limited memory capacity. The optimal model configurations for three datasets are given in Table 6 of the appendix.

**Ablation Studies on CompoundE Variants.** We conduct ablation studies on three variants of CompoundE; namely, CompoundE-Full, CompoundE-Head and CompoundE-Tail as described in Section 3.1. The goal is to determine the variant that performs the best on FB15k-237 and ogbl-wikikg2 datasets. Moreover, we test different ways of composing CompoundE by shuffling the order of translation, scaling, and rotation operations. Since geometric transformations are not commutative, different orders of cascading yield different models. Hence, we expect results for different CompoundE variants to be different. We present results of distinct CompoundE variants on ogbl-wikikg2 and FB15k-237 in Table 7 of the appendix. The main results are summarized here. For ogbl-wikikg2, the best performing scoring function is  $\|\mathbf{h} - \hat{\mathbf{S}} \cdot \hat{\mathbf{T}} \cdot \hat{\mathbf{R}} \cdot \mathbf{t}\|$  while the best performing scoring function for FB15k-237 is  $\|\mathbf{S} \cdot \mathbf{R} \cdot \mathbf{T} \cdot \mathbf{h} - \hat{\mathbf{S}} \cdot \hat{\mathbf{R}} \cdot \hat{\mathbf{T}} \cdot \mathbf{t}\|$ . For simplicity, we set the hyperparameters to be the same across experiments in all variants.

**Performance on Complex Relation Types.** To gain insights into the superior performance of CompoundE, we examine the performance of CompoundE on each type of relations. KG relations can be categorized into 4 types: 1) 1-to-1, 2) 1-to-N, 3) N-to-1, and 4) N-to-N. We can classify relations by counting the co-occurrence of their respective head and tail entities. A relation is classified as a 1-to-1 if each head entity can co-occur with at most one tail entity, 1-to-N if each head entity can co-occur with multiple tail entities, N-to-1 if multiple head entities can co-occur with the same tail entity, and N-to-N if multiple head entities can co-occur with multiple tail entities. We make decision based on the following rule. For each relation,  $r$ , we compute the average number of subject (head) entities per object (tail) entity as

$hpt_r$  and the average number of object entities per subject as  $tph_r$ . Then, with a specific threshold  $\eta$ ,

$$\begin{cases} hpt_r < \eta \text{ and } tph_r < \eta \implies r \text{ is 1-to-1} \\ hpt_r < \eta \text{ and } tph_r \geq \eta \implies r \text{ is 1-to-N} \\ hpt_r \geq \eta \text{ and } tph_r < \eta \implies r \text{ is N-to-1} \\ hpt_r \geq \eta \text{ and } tph_r \geq \eta \implies r \text{ is N-to-N.} \end{cases} \tag{20}$$

We set  $\eta = 1.5$  as a logical threshold by following the convention. Table 3 compares the MRR scores of CompoundE with benchmarking models on 1-to-1, 1-to-N, N-to-1, and N-to-N relations in head and tail entities prediction performance for the FB15k237 dataset. We see that CompoundE consistently outperforms benchmarking models in all relation categories. We show the performance of CompoundE on each relation type for the WN18RR dataset in Table 8 of the appendix. Generally, CompoundE has a significant advantage over benchmarking models for certain 1-N relations (e.g., “member\_of\_domain\_usage” and “member\_of\_domain\_region”) and for some N-1 relations (e.g., “synset\_domain\_topic\_of”). CompoundE is more effective than traditional KGE models in modeling complex relations.

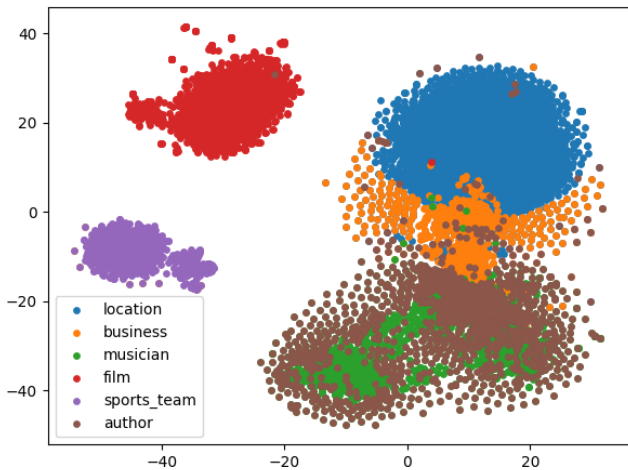


Figure 3:  $t$ -SNE visualization of entity embedding in the 2D space for some major entity types in FB15K-237.

Table 3: Filtered MRR on four relation types of FB15k-237.

Task Rel. Category	Predicting Head				Predicting Tail			
	1-to-1	1-to-N	N-to-1	N-to-N	1-to-1	1-to-N	N-to-1	N-to-N
TransE	0.492	0.454	0.081	0.252	0.485	0.072	0.740	0.367
RotatE	0.493	0.471	0.088	0.259	0.491	0.072	0.748	0.370
PairRE	0.496	0.476	0.117	0.274	0.492	0.073	0.763	0.387
CompoundE	<b>0.501</b>	<b>0.488</b>	<b>0.123</b>	<b>0.279</b>	<b>0.497</b>	<b>0.074</b>	<b>0.783</b>	<b>0.394</b>

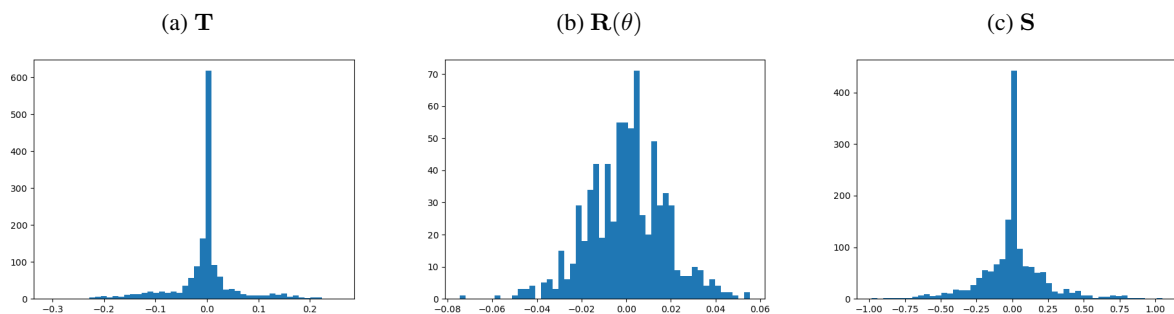
**Complexity Analysis.** We compare the computational complexity of CompoundE and several popular KGE models in Table 4. The last column gives the estimated number of free parameters used by different models to achieve the best performance for the ogbl-wikikg2 dataset. CompoundE cuts the number of parameters at least by half while achieving much better performance. In the table,  $n$ ,  $m$ , and  $d$  denote the entity number, the relation number, and their embedding dimension, respectively. Since  $n \gg m$  in most datasets, we can afford to increase the complexity of relation embedding for better link prediction result without significantly increasing the overall model complexity.

**Entity Semantics and Relation Component Values.** We provide a 2D  $t$ -SNE visualization of the entity embedding generated by CompoundE for FB15k-237 in Fig. 3. Each entity is colored with its respective entity type. As shown in the figure, some entity type class are well separated while others are not. This scatter plot shows that entity representations extracted by CompoundE can capture the semantics of the entity. Thus, their embeddings can be used in various downstream tasks such as KG entity typing and similarity based recommendations. In Fig. 4, we visualize



Table 4: Complexity comparison of KGE models.

Model	Ent. emb.	Rel. emb.	Scoring Function	Space	# Params
TransE	$\mathbf{h}, \mathbf{t} \in \mathbb{R}^d$	$\mathbf{r} \in \mathbb{R}^d$	$-\ \mathbf{h} + \mathbf{r} - \mathbf{t}\ _{1/2}$	$O((m+n)d)$	1251M
ComplEx	$\mathbf{h}, \mathbf{t} \in \mathbb{C}^d$	$\mathbf{r} \in \mathbb{C}^d$	$\text{Re}\left(\sum_{k=1}^K \mathbf{r}_k \mathbf{h}_k \bar{\mathbf{t}}_k\right)$	$O((m+n)d)$	1251M
RotatE	$\mathbf{h}, \mathbf{t} \in \mathbb{C}^d$	$\mathbf{r} \in \mathbb{C}^d$	$-\ \mathbf{h} \circ \mathbf{r} - \mathbf{t}\ $	$O((m+n)d)$	1250M
PairRE	$\mathbf{h}, \mathbf{t} \in \mathbb{R}^d$	$\mathbf{r}^{\mathbf{H}}, \mathbf{r}^{\mathbf{T}} \in \mathbb{R}^d$	$-\ \mathbf{h} \odot \mathbf{r}^{\mathbf{H}} - \mathbf{t} \odot \mathbf{r}^{\mathbf{T}}\ $	$O((m+n)d)$	500M
CompoundE-Head	$\mathbf{h}, \mathbf{t} \in \mathbb{R}^d$	$\mathbf{T}[:, d-1], \text{diag}(\mathbf{S}) \in \mathbb{R}^d, \theta \in \mathbb{R}^{d/2}$	$-\ \mathbf{T} \cdot \mathbf{R}(\theta) \cdot \mathbf{S} \cdot \mathbf{h} - \mathbf{t}\ $	$O((m+n)d)$	250.1M
CompoundE-Tail	$\mathbf{h}, \mathbf{t} \in \mathbb{R}^d$	$\hat{\mathbf{T}}[:, d-1], \text{diag}(\hat{\mathbf{S}}) \in \mathbb{R}^d, \theta \in \mathbb{R}^{d/2}$	$-\ \mathbf{h} - \hat{\mathbf{T}} \cdot \hat{\mathbf{R}}(\theta) \cdot \hat{\mathbf{S}} \cdot \mathbf{t}\ $	$O((m+n)d)$	250.1M
CompoundE-Full	$\mathbf{h}, \mathbf{t} \in \mathbb{R}^d$	$\mathbf{T}[:, d-1], \text{diag}(\mathbf{S}) \in \mathbb{R}^d, \theta \in \mathbb{R}^{d/2}$ $\hat{\mathbf{T}}[:, d-1], \text{diag}(\hat{\mathbf{S}}) \in \mathbb{R}^d$	$-\ \mathbf{T} \cdot \mathbf{R}(\theta) \cdot \mathbf{S} \cdot \mathbf{h} - \hat{\mathbf{T}} \cdot \hat{\mathbf{R}}(\theta) \cdot \hat{\mathbf{S}} \cdot \mathbf{t}\ $	$O((m+n)d)$	250.3M

Figure 4: Distribution of relation embedding values for “Friends” relation in FB15k-237, obtained using  $\|\mathbf{S}_r \cdot \mathbf{R}_r \cdot \mathbf{T}_r \cdot \mathbf{h} - \mathbf{t}\|$ 

relation embedding for the “friend” relation in FB15k-237 by plotting the histogram of translation, scaling, and rotation parameter values. Since “friend” is a symmetric relation, we expect the translation value to be close to zero, which is consistent with Fig. 4 (a). Also, since “friend” is an N-to-N relation, we expect the Compound operation to be singular. Actually, most of the scaling values are zero as shown in Fig. 4 (c). They support our theoretical analysis of CompoundE’s properties.

## 5 Conclusion and Future Work

A new KGE model called CompoundE was proposed in this work. We showed that quite a few distance-based KGE models are special cases of CompoundE. Extensive experiments were conducted for three datasets to demonstrate the effectiveness of CompoundE. CompoundE achieves state-of-the-art link prediction performance with a memory saving solution for large KGs. Visualization of entity semantics and relation embedding values was given to shed light on the superior performance of CompoundE.

We are interested in exploring two topics as future extensions. First, we may consider more complex operations in CompoundE. For example, there is a recent trend to extend 2D rotations to 3D rotations for rotation-based embeddings such as RotatE3D [47], SU2E [51]. It is worthwhile to explore CompoundE-3D. Second, CompoundE is expected to be useful in many downstream tasks. This conjecture has to be verified. If this is the case, CompoundE can offer a low memory solution to these tasks in realistic settings.

## References

- [1] Sören Auer, Christian Bizer, Georgi Kobilarov, Jens Lehmann, Richard Cyganiak, and Zachary Ives. DBpedia: A nucleus for a web of open data. In *The Semantic Web*, pages 722–735. 2007.
- [2] Fabian M Suchanek, Gjergji Kasneci, and Gerhard Weikum. YAGO: A core of semantic knowledge. In *Proc. 16th Int. Conf. World Wide Web (WWW’07)*, pages 697–706, 2007.
- [3] Andrew Carlson, Justin Betteridge, Bryan Kisiel, Burr Settles, Estevam R Hruschka, and Tom M Mitchell. Toward an architecture for never-ending language learning. In *Proc. 24th AAAI Conf. Artif. Intell.*, page 1306–1313, 2010.

- [4] Denny Vrandečić and Markus Krötzsch. Wikidata: a free collaborative knowledge base. *Commun. ACM*, 57(10):78–85, 2014.
- [5] Kurt Bollacker, Colin Evans, Praveen Paritosh, Tim Sturge, and Jamie Taylor. Freebase: a collaboratively created graph database for structuring human knowledge. In *Proc. 2008 ACM SIGMOD Int. Conf. Manage. Data (SIGMOD '08)*, pages 1247–1250, 2008.
- [6] Robyn Speer, Joshua Chin, and Catherine Havasi. ConceptNet 5.5: An open multilingual graph of general knowledge. In *Proc. 31st AAAI Conf. Artif. Intell.*, page 4444–4451, 2017.
- [7] Ying Shen, Ning Ding, Hai-Tao Zheng, Yaliang Li, and Min Yang. Modeling relation paths for knowledge graph completion. *IEEE Trans. Knowl. Data Eng.*, 33(11):3607–3617, 2020.
- [8] Zhengxiao Du, Chang Zhou, Jiangchao Yao, Teng Tu, Letian Cheng, Hongxia Yang, Jingren Zhou, and Jie Tang. CogKR: Cognitive graph for multi-hop knowledge reasoning. *IEEE Trans. Knowl. Data Eng.*, 2021.
- [9] Muhao Chen, Yingtao Tian, Mohan Yang, and Carlo Zaniolo. Multilingual knowledge graph embeddings for cross-lingual knowledge alignment. *arXiv preprint arXiv:1611.03954*, 2016.
- [10] Congcong Ge, Xiaoze Liu, Lu Chen, Baihua Zheng, and Yunjun Gao. LargeEA: Aligning entities for large-scale knowledge graphs. *Proc. 48th Int. Conf. Very Large Data Bases (VLDB'22)*, 15(2):237–245, 2022.
- [11] Xiou Ge, Yun-Cheng Wang, Bin Wang, and CC Jay Kuo. CORE: A knowledge graph entity type prediction method via complex space regression and embedding. *Pattern Recognit. Lett.*, 157:97–103, 2022.
- [12] William K Pratt. *Introduction to digital image processing*. CRC press, 2013.
- [13] George Wolberg. *Digital image warping*, volume 10662. IEEE Computer Society Press Los Alamitos, CA, 1990.
- [14] Steven M Seitz and Charles R Dyer. View morphing. In *Proc. 23rd Annu. Conf. Comput. Graphics Interactive Techniques (SIGGRAPH'96)*, pages 21–30, 1996.
- [15] Steven M LaValle. *Planning Algorithms*. Cambridge University Press, 2006.
- [16] Antoine Bordes, Nicolas Usunier, Alberto Garcia-Duran, Jason Weston, and Oksana Yakhnenko. Translating embeddings for modeling multi-relational data. *Adv. Neural Info. Process. Syst. 26 (NeurIPS 2013)*, page 2787–2795, 2013.
- [17] Zhiqing Sun, Zhi-Hong Deng, Jian-Yun Nie, and Jian Tang. Rotate: Knowledge graph embedding by relational rotation in complex space. In *Proc. 8th Int. Conf. Learn. Represent. (ICLR)*, page 1–18, 2019.
- [18] Linlin Chao, Jianshan He, Taifeng Wang, and Wei Chu. PairRE: Knowledge graph embeddings via paired relation vectors. In *Proc. 59th Annu. Meet. Assoc. Comput. Linguist. (ACL 2021)*, pages 4360–4369, August 2021.
- [19] Yanhui Peng and Jing Zhang. LineaRE: Simple but powerful knowledge graph embedding for link prediction. In *Proc. 2020 IEEE 20th Int. Conf. Data Min. (ICDM '20)*, pages 422–431, 2020.
- [20] Takuma Ebisu and Ryutaro Ichise. Generalized translation-based embedding of knowledge graph. *IEEE Trans. Knowl. Data Eng.*, 32(5):941–951, 2019.
- [21] Ivana Balažević, Carl Allen, and Timothy Hospedales. Multi-relational Poincaré graph embeddings. In *Adv. Neural Info. Process. Syst. 32 (NeurIPS 2019)*, volume 32, 2019.
- [22] Ines Chami, Adva Wolf, Da-Cheng Juan, Frederic Sala, Sujith Ravi, and Christopher Ré. Low-dimensional hyperbolic knowledge graph embeddings. In *Proc. 58th Annu. Meet. Assoc. Comput. Linguist. (ACL 2020)*, pages 6901–6914, 2020.
- [23] Maximilian Nickel, Volker Tresp, and Hans-Peter Kriegel. A three-way model for collective learning on multi-relational data. In *Proc. 28th Int. Conf. Mach. Learn. (ICML 2011)*, page 809–816, 2011.
- [24] Bishan Yang, Wen-tau Yih, Xiaodong He, Jianfeng Gao, and Li Deng. Embedding entities and relations for learning and inference in knowledge bases. In *Proc. 4th Int. Conf. Learn. Represent. (ICLR)*, pages 1–13, 2015.
- [25] Hanxiao Liu, Yuexin Wu, and Yiming Yang. Analogical inference for multi-relational embeddings. In *Proc. 34th Int. Conf. Mach. Learn. (ICML 2017)*, pages 2168–2178, 2017.
- [26] Théo Trouillon, Johannes Welbl, Sebastian Riedel, Éric Gaussier, and Guillaume Bouchard. Complex embeddings for simple link prediction. In *Proc. 33rd Int. Conf. Mach. Learn. (ICML 2016)*, pages 2071–2080, 2016.
- [27] Seyed Mehran Kazemi and David Poole. Simple embedding for link prediction in knowledge graphs. *Adv. Neural Info. Process. Syst. 31 (NeurIPS 2018)*, 31:4289–4300, 2018.
- [28] Ivana Balazevic et al. TuckER: Tensor factorization for knowledge graph completion. In *Proc. Conf. Empirical Meth. Natural Language Process. (EMNLP'19)*, pages 5185–5194, 2019.

- [29] Shuai Zhang, Yi Tay, Lina Yao, and Qi Liu. Quaternion knowledge graph embedding. In *Adv. Neural Info. Process. Syst. 32 (NeurIPS 2019)*, pages 2731–2741, 2019.
- [30] Zongsheng Cao, Qianqian Xu, Zhiyong Yang, Xiaochun Cao, and Qingming Huang. Dual quaternion knowledge graph embeddings. In *Proc. 35th AAAI Conf. Artif. Intell.*, pages 6894–6902, 2021.
- [31] Xin Dong, Evgeniy Gabrilovich, Jeremy Heitz, Wilko Horn, Ni Lao, Kevin Murphy, Thomas Strohmann, Shaohua Sun, and Wei Zhang. Knowledge vault: A web-scale approach to probabilistic knowledge fusion. In *Proc. 20th ACM SIGKDD Int. Conf. Knowl. Discov. Data Min. (KDD '14)*, pages 601–610, 2014.
- [32] Richard Socher, Danqi Chen, Christopher D Manning, and Andrew Ng. Reasoning with neural tensor networks for knowledge base completion. *Adv. Neural Info. Process. Syst. 26 (NeurIPS 2013)*, 26, 2013.
- [33] Tim Dettmers, Pasquale Minervini, Pontus Stenetorp, and Sebastian Riedel. Convolutional 2d knowledge graph embeddings. In *Proc. 32nd AAAI Conf. Artif. Intell.*, pages 1811–1818, 2018.
- [34] Michael Schlichtkrull, Thomas N Kipf, Peter Bloem, Rianne Van Den Berg, Ivan Titov, and Max Welling. Modeling relational data with graph convolutional networks. In *Proc. 15th Extended Semantic Web Conf. (ESWC'18)*, pages 593–607, 2018.
- [35] Shikhar Vashishth, Soumya Sanyal, Vikram Nitin, and Partha Talukdar. Composition-based multi-relational graph convolutional networks. In *Proc. 9th Int. Conf. Learn. Represent. (ICLR)*, 2020.
- [36] Zhaoli Zhang, Zhifei Li, Hai Liu, and Neal N Xiong. Multi-scale dynamic convolutional network for knowledge graph embedding. *IEEE Trans. Knowl. Data Eng.*, 34(5):2335–2347, 2022.
- [37] Yun-Cheng Wang, Xiou Ge, Bin Wang, and C-C Jay Kuo. KGBBoost: A classification-based knowledge base completion method with negative sampling. *Pattern Recognit. Lett.*, 157:104–111, 2022.
- [38] Zhen Wang, Jianwen Zhang, Jianlin Feng, and Zheng Chen. Knowledge graph embedding by translating on hyperplanes. In *Proc. 28th AAAI Conf. Artif. Intell.*, pages 1112–1119, 2014.
- [39] Yankai Lin, Zhiyuan Liu, Maosong Sun, Yang Liu, and Xuan Zhu. Learning entity and relation embeddings for knowledge graph completion. In *Proc. 29th AAAI Conf. Artif. Intell.*, pages 2181–2187, 2015.
- [40] Guoliang Ji, Shizhu He, Liheng Xu, Kang Liu, and Jun Zhao. Knowledge graph embedding via dynamic mapping matrix. In *Proc. 53rd Annu. Meet. Assoc. Comput. Linguist. (ACL 2015)*, volume 1, pages 687–696, 2015.
- [41] Guoliang Ji, Kang Liu, Shizhu He, and Jun Zhao. Knowledge graph completion with adaptive sparse transfer matrix. In *Proc. 30th AAAI Conf. Artif. Intell.*, pages 985–991, 2016.
- [42] Zongwei Liang, Junan Yang, Hui Liu, and Keju Huang. A semantic filter based on relations for knowledge graph completion. In *Proc. Conf. Empirical Meth. Natural Language Process. (EMNLP'21)*, pages 7920–7929, 2021.
- [43] Qianjin Zhang, Ronggui Wang, Juan Yang, and Lixia Xue. Knowledge graph embedding by reflection transformation. *Knowl.-Based Syst.*, 238:107861, 2022.
- [44] Zongsheng Cao, Qianqian Xu, Zhiyong Yang, Xiaochun Cao, and Qingming Huang. Geometry interaction knowledge graph embeddings. In *Proc. 36th AAAI Conf. Artif. Intell.*, 2022.
- [45] Takuma Ebisu and Ryutaro Ichise. Generalized translation-based embedding of knowledge graph. *IEEE Trans. Knowl. Data Eng.*, 32(5):941–951, 2019.
- [46] Yongqi Zhang, Quanming Yao, Wenyan Dai, and Lei Chen. Autosf: Searching scoring functions for knowledge graph embedding. In *Proc. 36th IEEE Int. Conf. Data Eng. (ICDE 2020)*, pages 433–444, 2020.
- [47] Chang Gao, Chengjie Sun, Lili Shan, Lei Lin, and Mingjiang Wang. Rotate3d: Representing relations as rotations in three-dimensional space for knowledge graph embedding. In *Proc. 29th ACM Int. Conf. Inf. Knowl. Manage. (CIKM'20)*, pages 385–394, 2020.
- [48] Jinxing Yu, Yunfeng Cai, Mingming Sun, and Ping Li. MQuade: a unified model for knowledge fact embedding. In *Proc. 30th Int. Conf. World Wide Web (WWW'21)*, pages 3442–3452, 2021.
- [49] Weihua Hu, Matthias Fey, Marinka Zitnik, Yuxiao Dong, Hongyu Ren, Bowen Liu, Michele Catasta, and Jure Leskovec. Open graph benchmark: Datasets for machine learning on graphs. *arXiv preprint arXiv:2005.00687*, 2020.
- [50] George A Miller. WordNet: a lexical database for english. *Commun. ACM*, 38(11):39–41, 1995.
- [51] Tong Yang, Long Sha, and Pengyu Hong. Nage: Non-Abelian group embedding for knowledge graphs. In *Proc. 29th ACM Int. Conf. Inf. Knowl. Manage. (CIKM'20)*, pages 1735–1742, 2020.

## 6 Appendix

### 6.1 Implementation and Optimal Configurations

The statistics of the three datasets used in our experiments are summarized in Table 5. In the experiments, we normalize all entity embeddings to unit vectors before applying compound operations. The optimal configurations of CompoundE are given in Table 6. The implementation of the rotation operation in the optimal CompoundE configuration for the WN18RR dataset is adapted from RotatE.

More experimental results are given in Fig. 5. The MRR scores of CompoundE under different batch sizes and negative sampling sizes for ogbl-wikikg2, FB15k-237, and WN18RR are shown in Figs. 5 (a)-(c), respectively. All experiments were conducted on a NVIDIA V100 GPU with 32GB memory. GPUs with larger memory such as NVIDIA A100 (40GB), NVIDIA A40 (48GB) are only needed for hyperparameter sweep when the dimension, the negative sample size, and the batch size are high. We should point out that such settings are not essential for CompoundE to obtain good results. They were used to search for the optimal configurations.

Table 5: Datasets Statistics

Dataset	#Entities	#Relations	#Training	#Validation	#Test
FB15k-237	14,541	237	272,115	17,535	20,466
WN18RR	40,943	11	86,835	3,034	3,134
ogbl-wikikg2	2,500,604	535	16,109,182	429,456	598,543

Table 6: Optimal Configurations

Dataset	CompoundE Variant	#Dim	$lr$	$B$	$N$	$\alpha$	$\zeta$
ogbl-wikikg2	$\ \mathbf{h} - \hat{\mathbf{S}} \cdot \hat{\mathbf{T}} \cdot \hat{\mathbf{R}} \cdot \mathbf{t}\ $	100	0.005	4096	250	1	7
FB15k-237	$\ \mathbf{S} \cdot \mathbf{R} \cdot \mathbf{T} \cdot \mathbf{h} - \hat{\mathbf{S}} \cdot \hat{\mathbf{R}} \cdot \hat{\mathbf{T}} \cdot \mathbf{t}\ $	1500	0.00005	1024	125	1	6
WN18RR	$\ \mathbf{R} \cdot \mathbf{S} \cdot \mathbf{T} \cdot \mathbf{h} - \hat{\mathbf{S}} \cdot \hat{\mathbf{T}} \cdot \mathbf{t}\ $	200	0.00005	1024	256	0.5	6

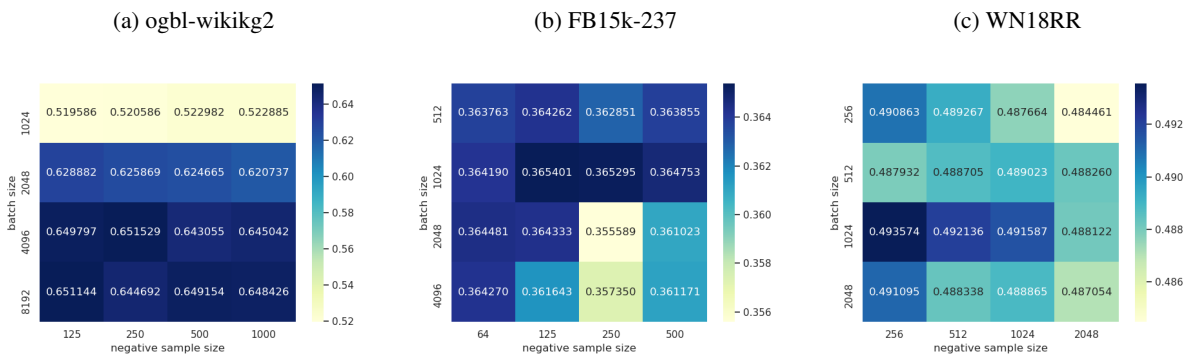


Figure 5: Heatmap of test MRR scores with a grid search for different combinations of batch sizes and negative sample sizes.

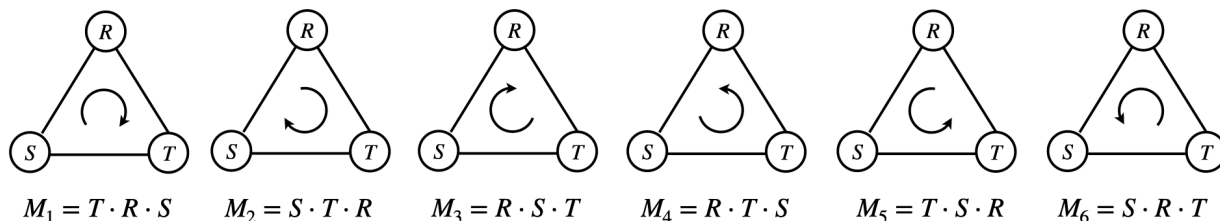


Figure 6: Illustration of different ways of composing compound operations.

## 6.2 Compositions of CompoundE

There are different ways to arrange the order of translation, rotation and scaling operations in CompoundE. They are summarized in Fig. 6. Furthermore, we report the link prediction performance of different compositions of CompoundE for ogbl-wikikg2 and FB15k-237 in Table 7. The best performing variant for ogbl-wikikg2 is  $\|\mathbf{h} - \hat{\mathbf{S}} \cdot \hat{\mathbf{T}} \cdot \hat{\mathbf{R}} \cdot \mathbf{t}\|$  and the second best is  $\|\mathbf{h} - \hat{\mathbf{T}} \cdot \hat{\mathbf{S}} \cdot \hat{\mathbf{R}} \cdot \mathbf{t}\|$ . The most effective variant for FB15k-237  $\|\mathbf{S} \cdot \mathbf{R} \cdot \mathbf{T} \cdot \mathbf{h} - \hat{\mathbf{S}} \cdot \hat{\mathbf{R}} \cdot \hat{\mathbf{T}} \cdot \mathbf{t}\|$  and the second best is  $\|\mathbf{T} \cdot \mathbf{S} \cdot \mathbf{R} \cdot \mathbf{h} - \hat{\mathbf{T}} \cdot \hat{\mathbf{S}} \cdot \hat{\mathbf{R}} \cdot \mathbf{t}\|$ .

## 6.3 Properties of CompoundE

Let  $\mathbf{M}$  and  $\hat{\mathbf{M}}$  denote the compound operation for the head and tail entity embeddings, respectively. In the following, we will prove nine properties of CompoundE.

**Proposition 6.1.** *CompoundE can model 1-N relations.*

*Proof.* A relation  $r$  is an 1-N relation iff there exist at least two distinct tail entities  $t_1$  and  $t_2$  such that  $(h, r, t_1)$  and  $(h, r, t_2)$  both hold. Then we have:

$$\begin{aligned} \mathbf{M} \cdot \mathbf{h} &= \hat{\mathbf{M}} \cdot \mathbf{t}_1, & \mathbf{M} \cdot \mathbf{h} &= \hat{\mathbf{M}} \cdot \mathbf{t}_2 \\ \hat{\mathbf{M}} \cdot (\mathbf{t}_1 - \mathbf{t}_2) &= 0 \end{aligned} \quad (21)$$

Since  $\mathbf{t}_1 \neq \mathbf{t}_2$ , CompoundE can model 1-N relations when  $\hat{\mathbf{M}}$  is singular.  $\square$

**Proposition 6.2.** *CompoundE can model N-1 relations.*

*Proof.* A relation  $r$  is an N-1 relation iff there exist at least two distinct head entities  $h_1$  and  $h_2$  such that  $(h_1, r, t)$  and  $(h_2, r, t)$  both hold. Then we have:

$$\begin{aligned} \mathbf{M} \cdot \mathbf{h}_1 &= \hat{\mathbf{M}} \cdot \mathbf{t}, & \mathbf{M} \cdot \mathbf{h}_2 &= \hat{\mathbf{M}} \cdot \mathbf{t} \\ \mathbf{M} \cdot (\mathbf{h}_1 - \mathbf{h}_2) &= 0 \end{aligned} \quad (22)$$

Since  $\mathbf{h}_1 \neq \mathbf{h}_2$ , CompoundE can model N-1 relations when  $\mathbf{M}$  is singular.  $\square$

**Proposition 6.3.** *CompoundE can model N-N relations.*

*Proof.* By the proof for Prop.6.1 and 6.2, N-N relations can be modeled when both  $\mathbf{M}$  and  $\hat{\mathbf{M}}$  are singular.  $\square$

**Proposition 6.4.** *CompoundE can model symmetric relations.*

*Proof.* A relation  $r$  is a symmetric relation iff  $(h, r, t)$  and  $(t, r, h)$  holds simultaneously. Then we have:

$$\begin{aligned} \mathbf{M} \cdot \mathbf{h} &= \hat{\mathbf{M}} \cdot \mathbf{t} \implies \mathbf{h} = \mathbf{M}^{-1} \hat{\mathbf{M}} \cdot \mathbf{t} \\ \mathbf{M} \cdot \mathbf{t} &= \hat{\mathbf{M}} \cdot \mathbf{h} \implies \mathbf{M} \cdot \mathbf{t} = \hat{\mathbf{M}} \mathbf{M}^{-1} \hat{\mathbf{M}} \cdot \mathbf{t} \\ \mathbf{M} \hat{\mathbf{M}}^{-1} &= \hat{\mathbf{M}} \mathbf{M}^{-1} \end{aligned} \quad (23)$$

Therefore, CompoundE can model symmetric relations when  $\mathbf{M} \hat{\mathbf{M}}^{-1} = \hat{\mathbf{M}} \mathbf{M}^{-1}$ .  $\square$

**Proposition 6.5.** *CompoundE can model antisymmetric relations.*

*Proof.* A relation  $r$  is a antisymmetric relation iff  $(h, r, t)$  holds but  $(t, r, h)$  does not. By similar proof for Proposition 6.4, CompoundE can model symmetric relations when  $\mathbf{M} \hat{\mathbf{M}}^{-1} \neq \hat{\mathbf{M}} \mathbf{M}^{-1}$ .  $\square$

**Proposition 6.6.** *CompoundE can model inversion relations.*

*Proof.* A relation  $r_2$  is the inverse of relation  $r_1$  iff  $(h, r_1, t)$  and  $(t, r_2, h)$  holds simultaneously. Then we have:

$$\begin{aligned} \mathbf{M}_1 \cdot \mathbf{h} &= \hat{\mathbf{M}}_1 \cdot \mathbf{t} \implies \mathbf{h} = \mathbf{M}_1^{-1} \hat{\mathbf{M}}_1 \cdot \mathbf{t} \\ \mathbf{M}_2 \cdot \mathbf{t} &= \hat{\mathbf{M}}_2 \cdot \mathbf{h} \implies \mathbf{M}_2 \cdot \mathbf{t} = \hat{\mathbf{M}}_2 \mathbf{M}_1^{-1} \hat{\mathbf{M}}_1 \cdot \mathbf{t} \\ \hat{\mathbf{M}}_2^{-1} \mathbf{M}_2 &= \mathbf{M}_1^{-1} \hat{\mathbf{M}}_1 \end{aligned} \quad (24)$$

Therefore, CompoundE can model inversion relations when  $\hat{\mathbf{M}}_2^{-1} \mathbf{M}_2 = \mathbf{M}_1^{-1} \hat{\mathbf{M}}_1$ .  $\square$

**Proposition 6.7.** *CompoundE can model transitive relations.*

*Proof.* A set of relations  $(r_1, r_2, r_3)$  are transitive iff  $(e_1, r_1, e_2)$ ,  $(e_2, r_2, e_3)$ , and  $(e_1, r_3, e_3)$  hold simultaneously. Then we have:

$$\begin{aligned}
 \mathbf{M}_1 \cdot \mathbf{e}_1 &= \hat{\mathbf{M}}_1 \cdot \mathbf{e}_2 \implies \mathbf{e}_1 = \mathbf{M}_1^{-1} \hat{\mathbf{M}}_1 \cdot \mathbf{e}_2 \\
 \mathbf{M}_2 \cdot \mathbf{e}_2 &= \hat{\mathbf{M}}_2 \cdot \mathbf{e}_3 \implies \mathbf{e}_3 = \hat{\mathbf{M}}_2^{-1} \mathbf{M}_2 \cdot \mathbf{e}_2 \\
 \mathbf{M}_3 \cdot \mathbf{e}_1 &= \hat{\mathbf{M}}_3 \cdot \mathbf{e}_3 \\
 \mathbf{M}_3 \mathbf{M}_1^{-1} \hat{\mathbf{M}}_1 \cdot \mathbf{e}_2 &= \hat{\mathbf{M}}_3 \hat{\mathbf{M}}_2^{-1} \mathbf{M}_2 \cdot \mathbf{e}_2 \\
 \hat{\mathbf{M}}_3^{-1} \mathbf{M}_3 &= (\hat{\mathbf{M}}_2^{-1} \mathbf{M}_2) (\hat{\mathbf{M}}_1^{-1} \mathbf{M}_1)
 \end{aligned}
 \tag{25}$$

Therefore, CompoundE can model transitive relations when  $\hat{\mathbf{M}}_3^{-1} \mathbf{M}_3 = (\hat{\mathbf{M}}_2^{-1} \mathbf{M}_2) (\hat{\mathbf{M}}_1^{-1} \mathbf{M}_1)$ . □

Table 7: Filtered ranking of link prediction for ogbl-wikikg2 and FB15k-237

Datasets	ogbl-wikikg2				FB15k-237			
	Model	MRR	Hit@1	Hit@3	Hit@10	MRR	Hit@1	Hit@3
$\ \mathbf{T} \cdot \mathbf{R} \cdot \mathbf{S} \cdot \mathbf{h} - \mathbf{t}\ $	0.6001	0.5466	0.6187	0.7043	0.3373	0.2455	0.3720	0.5217
$\ \mathbf{T} \cdot \mathbf{S} \cdot \mathbf{R} \cdot \mathbf{h} - \mathbf{t}\ $	0.5972	0.5431	0.6157	0.7002	0.3359	0.2467	0.3685	0.5171
$\ \mathbf{S} \cdot \mathbf{T} \cdot \mathbf{R} \cdot \mathbf{h} - \mathbf{t}\ $	0.6019	0.5459	0.6211	0.7091	0.3354	0.2461	0.3680	0.5169
$\ \mathbf{R} \cdot \mathbf{T} \cdot \mathbf{S} \cdot \mathbf{h} - \mathbf{t}\ $	0.5838	0.5288	0.6016	0.6880	0.3356	0.2456	0.3687	0.5167
$\ \mathbf{S} \cdot \mathbf{R} \cdot \mathbf{T} \cdot \mathbf{h} - \mathbf{t}\ $	0.6006	0.5460	0.6185	0.7043	0.3342	0.2449	0.3662	0.5141
$\ \mathbf{R} \cdot \mathbf{S} \cdot \mathbf{T} \cdot \mathbf{h} - \mathbf{t}\ $	0.5834	0.5239	0.6039	0.6979	0.3355	0.2460	0.3698	0.5165
$\ \mathbf{h} - \hat{\mathbf{T}} \cdot \hat{\mathbf{R}} \cdot \hat{\mathbf{S}} \cdot \mathbf{t}\ $	0.6440	0.5777	0.6688	0.7787	0.3326	0.2393	0.3681	0.5183
$\ \mathbf{h} - \hat{\mathbf{T}} \cdot \hat{\mathbf{S}} \cdot \hat{\mathbf{R}} \cdot \mathbf{t}\ $	<u>0.6497</u>	<u>0.5827</u>	<u>0.6758</u>	<u>0.7858</u>	0.3302	0.2384	0.3658	0.5123
$\ \mathbf{h} - \hat{\mathbf{S}} \cdot \hat{\mathbf{T}} \cdot \hat{\mathbf{R}} \cdot \mathbf{t}\ $	<b>0.6515</b>	<b>0.5844</b>	<b>0.6781</b>	<b>0.7873</b>	0.3313	0.2397	0.3680	0.5113
$\ \mathbf{h} - \hat{\mathbf{R}} \cdot \hat{\mathbf{T}} \cdot \hat{\mathbf{S}} \cdot \mathbf{t}\ $	0.6434	0.5779	0.6678	0.7763	0.3312	0.2394	0.3674	0.5136
$\ \mathbf{h} - \hat{\mathbf{S}} \cdot \hat{\mathbf{R}} \cdot \hat{\mathbf{T}} \cdot \mathbf{t}\ $	0.6474	0.5802	0.6739	0.7842	0.3290	0.2384	0.3640	0.5090
$\ \mathbf{h} - \hat{\mathbf{R}} \cdot \hat{\mathbf{S}} \cdot \hat{\mathbf{T}} \cdot \mathbf{t}\ $	0.6442	0.5777	0.6699	0.7788	0.3298	0.2383	0.3650	0.5114
$\ \mathbf{T} \cdot \mathbf{R} \cdot \mathbf{S} \cdot \mathbf{h} - \hat{\mathbf{T}} \cdot \hat{\mathbf{R}} \cdot \hat{\mathbf{S}} \cdot \mathbf{t}\ $	0.5479	0.4918	0.5661	0.6549	0.3426	0.2535	0.3770	0.5201
$\ \mathbf{T} \cdot \mathbf{S} \cdot \mathbf{R} \cdot \mathbf{h} - \hat{\mathbf{T}} \cdot \hat{\mathbf{S}} \cdot \hat{\mathbf{R}} \cdot \mathbf{t}\ $	0.5776	0.5210	0.5975	0.6852	<u>0.3613</u>	<u>0.2702</u>	<u>0.3948</u>	<u>0.5462</u>
$\ \mathbf{S} \cdot \mathbf{T} \cdot \mathbf{R} \cdot \mathbf{h} - \hat{\mathbf{S}} \cdot \hat{\mathbf{T}} \cdot \hat{\mathbf{R}} \cdot \mathbf{t}\ $	0.5782	0.5249	0.5962	0.6783	0.3597	0.2687	0.3937	0.5450
$\ \mathbf{R} \cdot \mathbf{T} \cdot \mathbf{S} \cdot \mathbf{h} - \hat{\mathbf{R}} \cdot \hat{\mathbf{T}} \cdot \hat{\mathbf{S}} \cdot \mathbf{t}\ $	0.5611	0.5053	0.5802	0.6660	0.3402	0.2506	0.3721	0.5213
$\ \mathbf{S} \cdot \mathbf{R} \cdot \mathbf{T} \cdot \mathbf{h} - \hat{\mathbf{S}} \cdot \hat{\mathbf{R}} \cdot \hat{\mathbf{T}} \cdot \mathbf{t}\ $	0.5736	0.5175	0.5918	0.6805	<b>0.3634</b>	<b>0.2718</b>	<b>0.3984</b>	<b>0.5500</b>
$\ \mathbf{R} \cdot \mathbf{S} \cdot \mathbf{T} \cdot \mathbf{h} - \hat{\mathbf{R}} \cdot \hat{\mathbf{S}} \cdot \hat{\mathbf{T}} \cdot \mathbf{t}\ $	0.5586	0.5057	0.5743	0.6592	0.3493	0.2593	0.3836	0.5301

Table 8: Filtered MRR on each relation type of WN18RR

Relation	Category	TransE	RotatE	CompoundE
similar_to	1-to-1	0.294	<b>1.000</b>	<b>1.000</b>
verb_group	1-to-1	0.363	0.961	<b>0.974</b>
member_meronym	1-to-N	0.179	<b>0.259</b>	0.230
has_part	1-to-N	0.117	<b>0.200</b>	0.190
member_of_domain_usage	1-to-N	0.113	0.297	<b>0.332</b>
member_of_domain_region	1-to-N	0.114	0.217	<b>0.280</b>
hypernym	N-to-1	0.059	<b>0.156</b>	0.155
instance_hypernym	N-to-1	0.289	0.322	<b>0.337</b>
synset_domain_topic_of	N-to-1	0.149	0.339	<b>0.367</b>
also_see	N-to-N	0.227	0.625	<b>0.629</b>
derivationally_related_form	N-to-N	0.440	<b>0.957</b>	0.956

**Proposition 6.8.** *CompoundE can model both both commutative and non-commutative relations.*

*Proof.* Since the general form of affine group is non-commutative, our proposed CompoundE is non-commutative i.e.

$$(\mathbf{M}_1 \hat{\mathbf{M}}_1^{-1}) (\mathbf{M}_2 \hat{\mathbf{M}}_2^{-1}) \neq (\mathbf{M}_2 \hat{\mathbf{M}}_2^{-1}) (\mathbf{M}_1 \hat{\mathbf{M}}_1^{-1})
 \tag{26}$$

where each  $\mathbf{M}$  consists of translation, rotation, and scaling component. However, in special cases, when our relation embedding has only one of the translation, rotation, or scaling component, then the relation embedding becomes commutative again.  $\square$

**Proposition 6.9.** *CompoundE can model sub-relations.*

*Proof.* A relation  $r_1$  is a sub-relation of  $r_2$  if  $(h, r_2, t)$  implies  $(h, r_1, t)$ . Without loss of generality, suppose our compounding operation takes the following form

$$\mathbf{M} = \mathbf{T} \cdot \mathbf{R} \cdot \mathbf{S}, \hat{\mathbf{M}} = \hat{\mathbf{T}} \cdot \hat{\mathbf{R}} \cdot \hat{\mathbf{S}}, \quad (27)$$

and suppose

$$\begin{aligned} \mathbf{T}_1 &= \mathbf{T}_2, \hat{\mathbf{T}}_1 = \hat{\mathbf{T}}_2, \\ \mathbf{R}_1 &= \mathbf{R}_2, \hat{\mathbf{R}}_1 = \hat{\mathbf{R}}_2, \\ \mathbf{S}_1 &= \gamma \mathbf{S}_2, \hat{\mathbf{S}}_1 = \gamma \hat{\mathbf{S}}_2, \gamma \leq 1. \end{aligned} \quad (28)$$

With these conditions, we can compare the CompoundE scores generated by  $(h, r_1, t)$  and  $(h, r_2, t)$  as follows:

$$\begin{aligned} & f_{r_1}(h, t) - f_{r_2}(h, t) \\ &= \|\mathbf{T}_1 \cdot \mathbf{R}_1 \cdot \mathbf{S}_1 \cdot \mathbf{h} - \hat{\mathbf{T}}_1 \cdot \hat{\mathbf{R}}_1 \cdot \hat{\mathbf{S}}_1 \cdot \mathbf{t}\| - \|\mathbf{T}_2 \cdot \mathbf{R}_2 \cdot \mathbf{S}_2 \cdot \mathbf{h} - \hat{\mathbf{T}}_2 \cdot \hat{\mathbf{R}}_2 \cdot \hat{\mathbf{S}}_2 \cdot \mathbf{t}\| \\ &= \|\mathbf{T}_2 \cdot \mathbf{R}_2 \cdot (\gamma \mathbf{S}_2) \cdot \mathbf{h} - \hat{\mathbf{T}}_2 \cdot \hat{\mathbf{R}}_2 \cdot (\gamma \hat{\mathbf{S}}_2) \cdot \mathbf{t}\| - \|\mathbf{T}_2 \cdot \mathbf{R}_2 \cdot \mathbf{S}_2 \cdot \mathbf{h} - \hat{\mathbf{T}}_2 \cdot \hat{\mathbf{R}}_2 \cdot \hat{\mathbf{S}}_2 \cdot \mathbf{t}\| \\ &= \|\gamma(\mathbf{T}_2 \cdot \mathbf{R}_2 \cdot \mathbf{S}_2 \cdot \mathbf{h} - \hat{\mathbf{T}}_2 \cdot \hat{\mathbf{R}}_2 \cdot \hat{\mathbf{S}}_2 \cdot \mathbf{t})\| - \|\mathbf{T}_2 \cdot \mathbf{R}_2 \cdot \mathbf{S}_2 \cdot \mathbf{h} - \hat{\mathbf{T}}_2 \cdot \hat{\mathbf{R}}_2 \cdot \hat{\mathbf{S}}_2 \cdot \mathbf{t}\| \leq 0 \end{aligned} \quad (29)$$

This means that  $(h, r_1, t)$  generates a smaller error score than  $(h, r_2, t)$ . If  $(h, r_2, t)$  holds,  $(h, r_1, t)$  must also hold. Therefore,  $r_1$  is a sub-relation of  $r_2$ .  $\square$

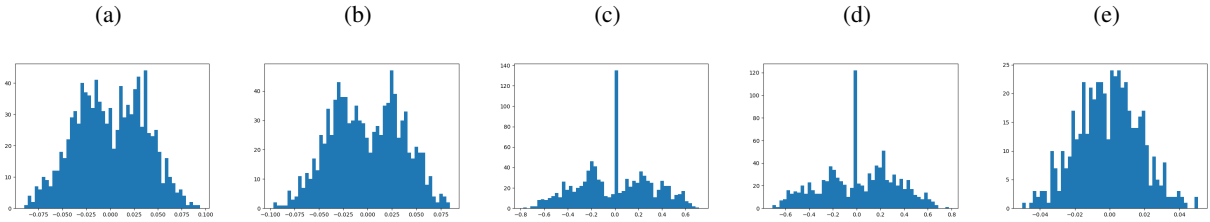


Figure 7: FB15k-237 “Friends” relation embedding obtained using  $\|\mathbf{S} \cdot \mathbf{R} \cdot \mathbf{T} \cdot \mathbf{h} - \hat{\mathbf{S}} \cdot \hat{\mathbf{R}} \cdot \hat{\mathbf{T}} \cdot \mathbf{t}\|$ : (a) distribution of head translation values, (b) distribution of tail translation values, (c) distribution of head scaling values, (d) distribution of tail scaling values, and (e) distribution of rotation angle values.

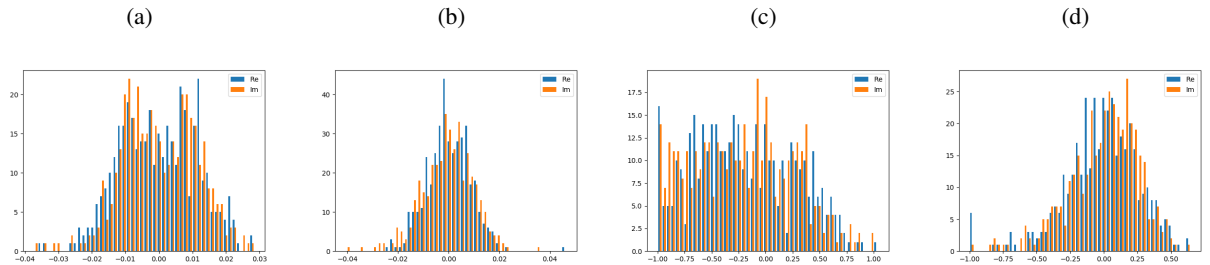


Figure 8: WN18RR “instance\_hypernym” relation: (a) distribution of head translation values, (b) distribution of tail translation values, (c) distribution of head scaling values, and (d) distribution of tail scaling values.

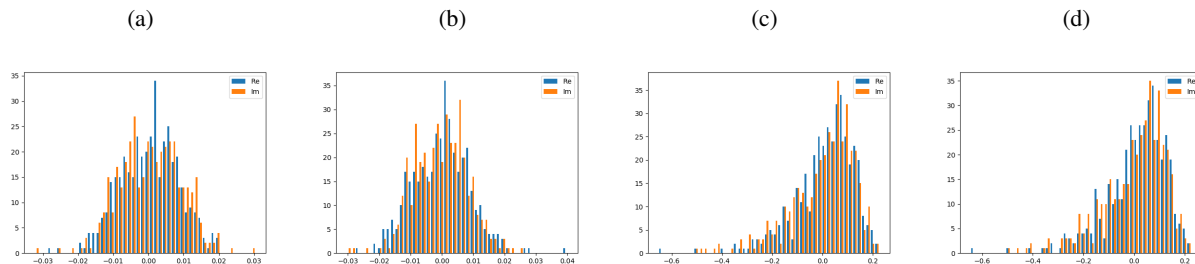


Figure 9: WN18RR “similar\_to” relation: (a) distribution of head translation values, (b) distribution of tail translation values, (c) distribution of head scaling values, and (d) distribution of tail scaling values.

#### 6.4 Complex Relation Modeling and Histograms of Embedding Values

The filtered MRR scores on each relation type of WN18RR are given in Table 8. We see that CompoundE has a significant advantage over benchmarking models for certain 1-N relations such as “member\_of\_domain\_usage” (+11.8%) and “member\_of\_domain\_region” (+29.0%) and for some N-1 relations such as “synset\_domain\_topic\_of” (+8.3%).

Besides the histograms shown in the main paper, we add more plots to visualize CompoundE relation embedding values. In Fig. 7, we show the embedding values for the “Friends” relation in the FB15k-237. We use the CompoundE-full variant ( $\|\mathbf{S}_r \cdot \mathbf{R}_r \cdot \mathbf{T}_r \cdot \mathbf{h} - \hat{\mathbf{S}}_r \cdot \hat{\mathbf{R}}_r \cdot \hat{\mathbf{T}}_r \cdot \mathbf{t}\|$ ) to generate the embedding. We plot the translation and scaling components for both the head and the tail. We only show a single plot for the rotation component since the rotation parameter is shared between the head and the tail. Different from the CompoundE-head ( $\|\mathbf{S}_r \cdot \mathbf{R}_r \cdot \mathbf{T}_r \cdot \mathbf{h} - \mathbf{t}\|$ ), we see two modes (instead of only one mode) in CompoundE-full’s plots. One conjecture for this difference is that CompoundE-full has a pair of operations on both the head and the tail, the distribution of values need to have two modes to maintain the symmetry. Similar to CompoundE-head, the scaling parameters of CompoundE-full have a large amount of zeros to maintain the singularity of compounding operators and help learn the N-to-N complex relations.

Fig. 8 and Fig. 9 display the histogram of relation embeddings for “instance\_hypernym” relation and “similar\_to” relation in WN18RR, respectively. The real (in blue) and the imaginary (in orange) parts are overlaid in each plot. Notice that “instance\_hypernym” is an antisymmetric relation while “similar\_to” is a symmetric relation. This relation pattern is reflected on the embedding histogram since the translation and the scaling histograms for the head and the tail are different in “instance\_hypernym”. In contrast, the translation and scaling histograms for the head and the tail are almost identical in “similar\_to”.